Front. Earth Sci. 2022, 16(3): 774–785
https://doi.org/10.1007/s11707-021-0933-6

RESEARCH ARTICLE

Seasonal variations of leaf wax *n*-alkane distributions and δ^2H values in peat-forming vascular plants from the Dajiuhu peatland, central China

Jiantao XUE (✉)[1], Xueying ZHANG[1], Jinzhi LI[1], Zhiqi ZHANG[2], Huaiying YAO[1,3]

1 Research Center for Environmental Ecology and Engineering, School of Environmental Ecology and Biological Engineering, Wuhan Institute of Technology, Wuhan 430073, China
2 Administration of Dajiuhu National Wetland Park of Shennongjia, Shennongjia 442417, China
3 Key Laboratory of Urban Environment and Health, Institute of Urban Environment, Chinese Academy of Sciences, Xiamen 361021, China

Abstract Leaf wax *n*-alkane compositions have been widely applied to reconstruct paleoclimate histories in peat deposits, yet understanding of how the *n*-alkanes vary during seasonal plant growth remains limited. Here we report variations in the molecular and wax-derived *n*-alkane hydrogen isotope (δ^2H_{alk}) in the three dominant vascular plant species (*Sanguisorba officinalis*, *Carex argyi*, *Euphorbia esula*) and surface peat deposits nearby from the Dajiuhu peatland over a growing season. All three species show a relatively high carbon preference index (CPI) in the beginning of the growing season, with the CPI values reaching as high as 50 in two of the three species. Two species (*S. officinalis*, *E. esula*) display relatively stable average chain length (ACL) values over the four sampling intervals, with standard derivations of 0.2–0.3. In contrast, *C. argyi* exhibits a significant fluctuation of ACL values (averaging 28.1±1.4) over the growing season. The δ^2H_{alk} in all three species decreased during leaf growth. In the final stage of growth, the δ^2H_{alk} values of the three species are similar to those in the surface peats collected from the peatland. Combining the results of our measurements of alkane concentration and δ^2H values, it is likely that *de novo* synthesis of leaf wax *n*-alkanes in the peat-forming plant species is mainly at the early stage of leaf development. In the following months, the removal process exceeds renewal, resulting in a general decrease of the concentration of the total *n*-alkanes and the integrated δ^2H_{alk} values. Thus the δ^2H_{alk} values probably integrate the environmental variations at the end of the plant growth period rather than the whole period or the early growth period. These results are significant and have the potential to improve the utility of δ^2H_{alk} values in paleoenvironmental reconstructions.

Keywords peat-forming vascular plants, *n*-alkanes, δ^2H ratio, seasonal variations, central China

1 Introduction

Peatlands provide important archives for Holocene paleoecology and paleoclimate reconstructions (Chambers et al., 2012; Blackford, 2000). Researchers have applied a variety of proxies to paleoenvironmental reconstructions based on peat sequences, including pollen, phytolith, testate amoebae, the humification index, and carbon and oxygen isotopic compositions of cellulose (e.g., Hong et al., 2001; Chambers et al., 2012; Qin et al., 2012; Yu et al., 2012; Song et al., 2014; Liu et al., 2020). Because the waterlogged, nutrient poor, and acidic conditions in peatlands favor organic matter accumulation (Rydin and Jeglum, 2006; Gogo et al., 2016), a variety of organic geochemical proxies have also been used (e.g., Cisneros-Dozal et al., 2010; Andersson et al., 2012). In particular, the high content of organic matter in peat deposits has attracted increasingly more attention to the study of molecular paleoclimate proxies. Long-chain *n*-alkanes are synthesized as part of leaf waxes by some peat-forming plants and are widely used as plant biomarkers. Their distributions discriminate between vegetation types, which prompt their application in paleoenvironmental reconstruction. For example, the hydrocarbons in the waxy coatings of *Sphagnum* species are commonly dominated by medium chain length *n*-C_{23} and *n*-C_{25} alkanes (e.g., Baas et al., 2000; Nott et al., 2000; Nichols et al., 2006; Bingham et al., 2010), whereas those of the angiosperm vascular plants in peatlands are dominated by longer chain *n*-

Received February 17, 2021; accepted July 26, 2021

E-mail: xuejiantaocug@163.com

alkanes, mainly *n*-C_{29} and *n*-C_{31} (Pancost et al., 2002; Nichols et al., 2006). In addition, previous studies have applied the leaf wax lipid-derived proxies for paleoenvironmental reconstructions during the Holocene epoch (e.g., Zhou et al., 2005; Ortiz et al., 2010; Nichols et al., 2014; Zheng et al., 2014; Huang et al.,2018a, 2018b).

The hydrogen isotopic compositions of leaf waxes have been shown to be very sensitive to paleohydrological conditions in continental settings (Sachse et al., 2012; Bai et al., 2015; Sessions, 2016; Huang et al., 2018a; Yan et al., 2020). The availability of water is an important controller for the initiation and lateral expansion of peat deposits. Consequently, δ^2H_{alk} values have been investigated in global peatlands (Xie et al., 2000; Seki et al., 2009, 2011; Nichols et al., 2010, 2012; Freimuth et al., 2019; Huang et al., 2018a, 2018b; Xia et al., 2020; Yan et al., 2020). The results of these studies reveal that δ^2H_{alk} values in peat deposits are sensitive to climate changes on centennial to millennial timescales. An important constraint for further applications of δ^2H_{alk} sequences on peat deposits to paleoclimatic reconstructions is our poor knowledge about the seasonal variations of δ^2H_{alk} values and the associated controls in peat settings. Previous investigations have studied how environmental factors affect δ^2H_{alk} values of grasses (Sessions, 2006; Sachse et al., 2010; Bai et al., 2019; Yang and Huang, 2020) and trees (Pedentchouk et al., 2008; Sachse et al., 2009, 2015; Kahmen et al., 2011; Tipple et al., 2013; Newberry et al., 2015; Huang et al., 2018c). In addition, it has been shown that the variations of δ^2H_{alk} values may also depend on plant type. Previous studies found that biosynthetic fractionation may vary up to 60 ‰ among different species (Kahmen et al., 2013a, 2013b). Hence, the δ^2H_{alk} values and the fractionations ($\varepsilon_{alk/sw}$) that occur from source water (δ^2H_{sw}) to leaf wax *n*-alkane may in turn indicate the changes in plant taxonomies. Based on integrated analysis of a series of data on plant δ^2H_{alk}, Liu et al. (2016) suggested that the δ^2H_{alk} and $\varepsilon_{alk/sw}$ values can be used to distinguish monocotyledons from dicotyledons on a global scale. In addition, the variations of δ^2H_{alk} and $\varepsilon_{alk/sw}$ values may be responding in part to season and timing of plant growth. Liu et al. (2017) demonstrated that the δ^2H_{alk} values were 20 ‰ ^{2}H-enriched in spring compared to that in autumn in a wood forest system. His other study found that the δ^2H_{alk} values are stable during the sampling period in an arid mountainous transect (Liu et al., 2021a), indicating the discrepancy in seasonal variations of δ^2H_{alk} values between different ecosystems. However, to the best of our knowledge, no one has reported the seasonal variations of leaf waxes and δ^2H_{alk} values in peat-forming plants (Freimuth et al., 2019). Better understandings of the main phase of leaf wax development and the associated seasonal origin of the δ^2H_{alk} signal will improve reconstructions of past climate changes in peatlands that utilize leaf waxes as paleohydrologic proxies.

Here we report the seasonal variations of leaf wax *n*-alkanes in the three dominant peat-forming plant species (two forbs and one grass) and surface peat deposits nearby in the Dajiuhu peatland, central China. The objectives of this study are to investigate the pattern of the seasonal variations of δ^2H_{alk} values in peat-forming conditions and to assess how they impact paleohydrologic reconstructions based on biomarker δ^2H_{alk} values.

2 Materials and methods

2.1 Sampling

Samples of peat-forming vegetation were collected from the Dajiuhu Peatland (31°28'N, 110°00'E; 1700 m above sea level), which is located in the Shennongjia Forestry Region, Hubei Province, central China. This peatland has developed in a sub-alpine closed basin and extends over an area of 16 km^2 (Fig. 1). The local climate is dominated by the East Asian Monsoon and has an annual mean rainfall of 1560 mm and an annual mean temperature of 7.2°C. The monthly mean precipitation and temperature during the sampling time were obtained from records of the Dajiuhu National Wetland Park. Both ambient temperature and local precipitation peak during the summer under the influence of the monsoonal climate (Fig. 2).

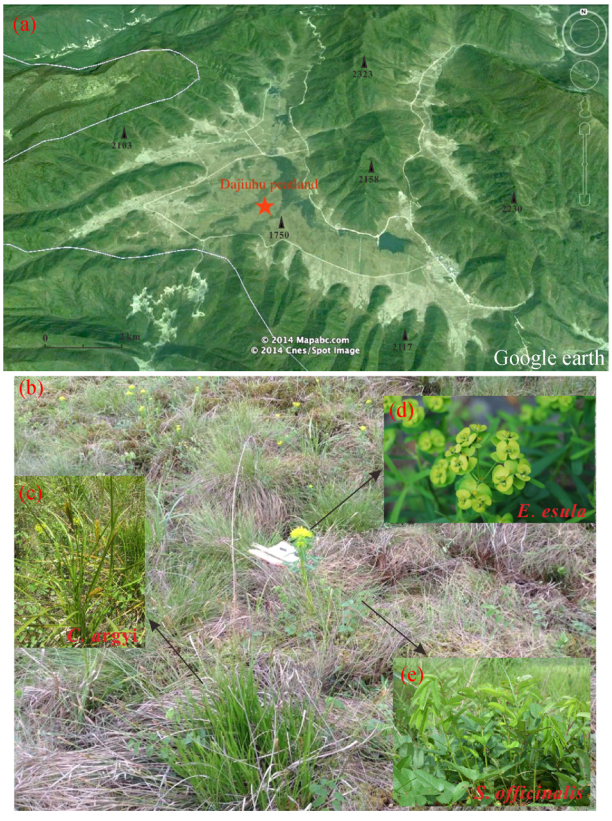

Fig. 1 (a) Image of the Dajiuhu peatland (downloaded from Google Earth); (b) live action photo taken on dajiuhu peatland; (c), (d), and (e) pictures of plants downloaded from the internet.

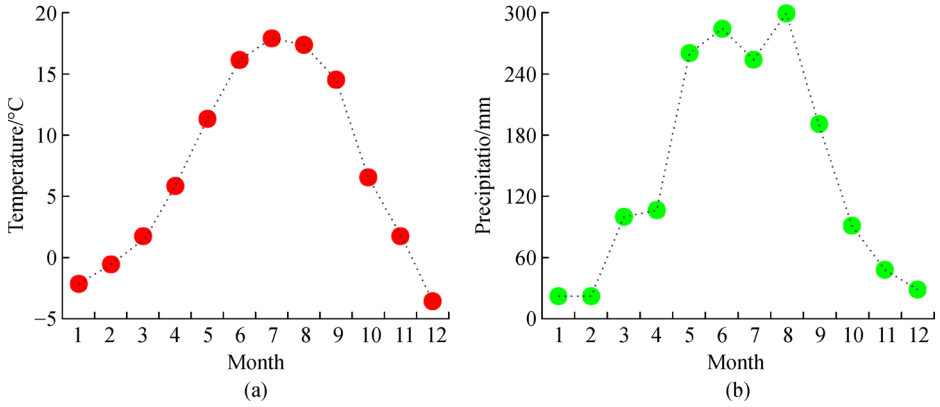

Fig. 2 (a) Monthly mean precipitation (MMP) and (b) mean air temperature (MAT) in Dajiuhu National Wetland Park during 2010.

A plant survey conducted in July 2012 showed that *Carex spp.* (sedges), *Sanguisorba officinalis* (great burnet), and *Euphorbia esula* (leafy spurge) were the dominant vascular plant species, together with the predominance of *Sphagnum palustre* (bog moss) in mosses (Luo et al., 2015). We selected *Carex argyi, S. officinalis* and *E. esula* as the representative vascular plant species to investigate the seasonal variations of δ^2H_{alk} values. Leaves of *C. argyi, S. officinalis* and *E. esula* were collected every two months during 2010 (May, July, September, November). Due to the cool temperatures of the relatively high altitude in the Dajiuhu basin, vascular plants normally bud in May. The samples collected in November were senescent leaves, still hanging on the shoots. During each field excursion, leaves of the three species were collected from at least 10 specimens of each species and combined to yield an averaged sample of each species. We also combined the δ^2H_{alk} values of the three plants collected in August 2017 for discussion (Huang et al., 2018a). In addition, a batch of surface peat deposits (0–2 cm) and surface peat waters were collected every two months during 2014 (May, July, September, November) from the same site where leaves were collected in 2010. These surface peat deposits were analyzed for their δ^2H_{alk} values as a comparison. The hydrogen isotopic compositions of peat source waters in surface 0–10 cm (δ^2H_{sw}) in 2014 were also analyzed to infer the δ^2H values of precipitation using an IWA-35-EP Liquid Water Analyzer with the same method described by Zhao et al. (2018).

2.2 Lipid extraction

Plant samples were washed with deionized water, air-dried, and cut into small pieces. Then the plant samples were ultrasonically extracted four times with CH_2Cl_2/methanol (9:1, volume/volume). An internal standard of cholane (Chiron, Norway) was added before extraction. The combined extracts were fractionated into aliphatic, aromatic, and polar fractions using silica gel column chromatography with hexane, CH_2Cl_2, and methanol as eluting solvents, respectively. The procedures for peat samples were similar with the above pretreatments and have been described in detail in Huang et al. (2014) and Zhao et al. (2018).

2.3 Instrumental analyses

The aliphatic fraction containing *n*-alkanes was quantified using a Shimadzu GC-2010 gas chromatograph (GC) equipped with a flame ionization detector (FID) and a DB-5 column (30 m × 0.25 mm i.d., 0.25 μm film thickness). The sample was injected in splitless mode with the injector temperature at 300°C. The oven temperature was initiated at 70°C and held for 1 min, then ramped to 210°C at a rate of 10°C·min^{-1}, and finally ramped to 300°C at a rate of 3°C·min^{-1} and kept isothermal for 25 min. A laboratory testing standard (mixture, *n*-C_{20}, *n*-C_{22}, *n*-C_{23}, *n*-C_{25}, *n*-C_{27}, *n*-C_{29}, *n*-C_{31}, *n*-C_{33} alkanes) was used to confirm peak time for *n*-alkanes and to calculate response factors of each *n*-alkane. The absolute abundances were calculated by comparison of peak areas with the internal standard and adjusted with the relevant response factors.

Compound-specific hydrogen isotope compositions of *n*-alkanes were determined using a Delta V advantage isotope ratio mass spectrometer coupled with a Trace GC and GC isolink. The GC oven temperature was initiated at 50°C and held for 1 min, and then ramped to 210°C at a rate of 10°C·min^{-1} (kept 2 min), and further ramped to 300°C at a rate of 6°C·min^{-1} (held 2 min), and finally ramped to 310°C at a rate of 10°C·min^{-1} and kept isothermal for 25 min. The high temperature conversion (HTC) system was operated at 1400°C. The HTC tube (HTC-reactor tube f.H_2, Thermofisher) was conditioned with methane. During the sample running interval, the H_3^+ factor varied between 3.10 and 3.30. To check the system stability, an Indiana reference mixture (A4, *n*-$C_{16–30}$ alkanes) with known δ^2H values was run between every two samples. Squalane ($\delta^2H = -167$ ‰) was used as the internal standard. Standard deviation for hydrogen isotope analysis was smaller than 5 ‰, based on at least duplicate analyses. The plant and peat samples were also performed duplicate analyses in the same time period. If the standard

deviation of two consecutive analyses was greater than 5‰, a third or more measurements were performed to verify the reliability of the data. Results are reported in the delta notation (‰) relative to Vienna Standard Mean Ocean Water (VSMOW) standard.

We use the measured δ^2H values of peat surface water (0–10 cm) to calculate the hydrogen isotope fractionations that occur from peat source water (δ^2H_{sw}) to long chain *n*-alkane ($\varepsilon_{alk/sw}$; Eq. (1)).

$$\varepsilon_{alk/sw} = 1000 \times \left(\frac{\delta^2H_{alk} + 1000}{\delta^2H_{sw} + 1000} - 1\right). \quad (1)$$

2.4 Date analyses

We conducted the Person correlations between the δ^2H_{sw}, δ^2H_{alk}, $\varepsilon_{alk/sw}$ and environmental factors (MAT and MMP). One-way ANOVA tests were performed to identify the significant differences among different plant types at the significance of 0.05 using the IBM SPSS Statistics.

3 Results

3.1 Variations of leaf wax *n*-alkane concentrations and alkane ratios

The chain lengths of the dominant *n*-alkanes in the three plant species range from C_{23} to C_{33}, and the total concentration of the C_{23} to C_{33} *n*-alkanes in the 12 plant samples varies between 17.7 and 1019.4 μg/g dry weight (Table 1). These results are in the ranges of previous studies of plants in the Dajiuhu peatland (Huang et al., 2011, 2014; Zhao et al., 2018).

In each of the three species, the alkane concentration changes over the growing season, and sometimes the difference can reach one order of magnitude (Fig. 3). The young leaves of the three species in May contain higher concentrations of *n*-alkanes than their more mature counterparts collected in July and September. At the end of the growing season (November), the leaf samples of *S. officinalis* and *E. esula*, but not *C. argyi*, show an obvious increase in *n*-alkane concentration relative to the earlier seasons (Fig. 3). In contrast, *C. argyi* leaves display a general decreasing trend in *n*-alkane concentration from May to November.

In addition to the variations of concentrations of total long chain *n*-alkanes in the leaf samples, the *n*-alkane molecular distributions change during the annual growth of the three species (Fig. 3). We use two *n*-alkane ratios, the carbon preference index (CPI; Marzi et al., 1993; Rao et al., 2009; Herrera-Herrera et al., 2020) and the average chain length (ACL; Poynter et al., 1989; Norström et al., 2017), to summarize the *n*-alkane changes. The CPI values in the plant samples show a sharp decrease from May to July and a further reduction to September (Fig. 3). The *n*-alkane CPI values calculated from the data in Chikaraishi and Naraoka (2006) similarly display a decreasing trend

Table 1 The concentration (μg/g dry weight), CPI, ACL values, and δ^2H_{alk} values (‰; standard deviation at least duplicate analyses shown in the parentheses) of leaf wax *n*-alkanes in the peat-forming plants collected from the Dajiuhu peatland at May, July, September, and November 2010

	Sanguisorba officinalis				*Euphorbia esula*				*Carex argyi*			
	May	July	September	November	May	July	September	November	May	July	September	November
n-C_{23}	0.8	0.7	1.9	2.6	3	2.5	0.1	4	8.7	4.3	8.4	0.8
n-C_{24}	0.4	0.7	2.7	1.7	0.4	0.8	0.2	2.3	1.9	0.8	2.3	0.1
n-C_{25}	4.4	3.9	7	9.7	27.6	16.9	1.4	28.1	26.5	8.7	32.9	1.2
n-C_{26}	1.1	1.3	6.8	3.4	2	4.5	1.5	17.6	2	0.8	1.2	0.2
n-C_{27}	16.7	10.7	21.6	48.9	80.4	50.5	4.1	117	44.7	9.7	8.1	2.8
n-C_{28}	0.9	7.6	9.1	4	0.4	6.5	2.1	33.4	2.5	1.1	0.5	0.5
n-C_{29}	53	22.5	23.3	56.2	20	28.6	3.3	94.3	53.1	21	9	9.7
n-C_{30}	1.7	4.3	4.7	9.2	0.6	2.4	0.6	11.1	1.8	1.4	0.3	0.7
n-C_{31}	253.1	114	75.6	225.9	62.5	69.7	2.8	92.1	26.7	14	6.9	11.2
n-C_{32}	8.5	7.3	5.1	13.3	0.7	0.9	0.1	2.3	0.7	0.5	0.4	0.5
n-C_{33}	533.9	303.9	188.5	644.4	40.7	34.4	1.5	51.5	3.5	3.3	2.5	3.5
CPI	47.2	14.3	7.8	21	51.2	12.2	2.8	5.4	17.6	12.3	13.5	13
ACL	32	32.1	31.6	31.9	29	29.5	28.8	29.1	27.9	28.4	26.4	29.7
δ^2H_{27}	–159(5)	–174(1)	–182(2)	–206(6)	–171(2)	–191(0)	–229(2)	–211(2)	–176(2)	–210(2)	–195(7)	–242(0)
δ^2H_{29}	–149(3)	–189(0)	–184(4)	–204(1)	–171(5)	–186(1)	–218(2)	–221(0)	–194(2)	–201(3)	–208(4)	–221(0)
δ^2H_{31}	–131(3)	–179(4)	–179(2)	–217(1)	–177(1)	–191(0)	–212(0)	–216(1)	–151(3)	–194(3)	–189(8)	–217(2)

Notes: $CPI = \frac{1}{2} \times \left(\frac{C_{23}+C_{25}+C_{27}+C_{29}+C_{31}}{C_{24}+C_{26}+C_{28}+C_{30}+C_{32}} + \frac{C_{25}+C_{27}+C_{29}+C_{31}+C_{33}}{C_{24}+C_{26}+C_{28}+C_{30}+C_{32}}\right)$; $ACL = (\sum_{odd} C_n \times n)/\sum_{odd} C_n$.

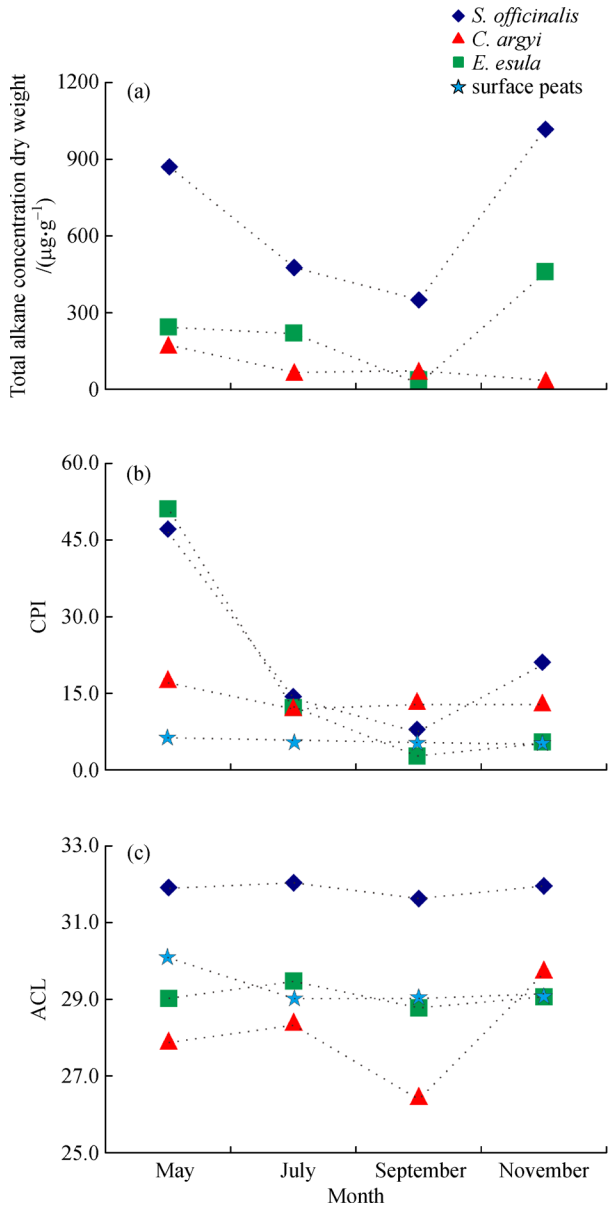

Fig. 3 (a) Variations of the total concentration (μg/g dry weight) and (b) CPI and (c) ACL values of the plant leaves and surface peat deposits over the sampling period in the Dajiuhu peatland.

from spring to autumn in two tree species. Huang et al. (2018c) also carried out a three-year monitoring project on two subtropical deciduous and showed the same phenomenon with the decreasing of CPI values in each natural year. This pattern may indicate that plants continually renew and replace their waxes through the growing seasons (Gao et al., 2012a, 2012b). Unlike the CPI values in the plant samples, the CPI values of surface peat deposit samples collected in different seasons have little variation (Fig. 3). Generally speaking, the CPI features in soil and sediments were inherited from overlying plants. The CPI values in the surface peat deposit samples were smaller than that in the plant samples collected in all seasons due to the enhanced microbial degradation in the peat deposits (Luo et al., 2012; Bush and McIerney, 2013).

The ACL values of the plant samples range from 26.4 to 32.1 (Fig. 3). Leaves of *S. officinalis* collected in July have the highest ACL value (32.1), whereas those of *C. argyi* in September have the lowest one (26.4). These three herb species, although growing in quite similar settings, show rather different averaged ACL values in 2010, which supports the previous conclusions that chemotaxonomic distinctions based on the maximal component (C_{max}) of leaf wax *n*-alkanes among plants should be made with caution (Rao et al., 2011; Bush and McInerney, 2013).

Through the growing season in 2010, *S. officinalis* and *E. esula* leaves show nearly constant ACL values, with a small variation of 0.5–0.7 unit (Fig. 3). In contrast, the ACL values of *C. argyi* show a small increase from May to July and then a major decrease to August and finally an increase of 3.3 from September to November (Table 2). The ACL values of the surface peat deposit samples in 2014 were similar in July, September, and November but slightly higher in May (Table 2 and Fig. 3).

3.2 Seasonal variations of δ^2H_{alk} and $\varepsilon_{alk/sw}$

We limit presentation to the *n*-alkane δ^2H values of *n*-C_{27}, *n*-C_{29}, and *n*-C_{31} because the concentrations of only these three compounds were sufficient for $^2H/^1H$ analyses in all the plant and peat samples (Table 1 and Table 2). From May to November, the δ^2H values of *n*-C_{27}, *n*-C_{29}, and *n*-C_{31} alkanes in *S. officinalis* range from −131 ‰ to −206 ‰, showing a consistently increasing level of ^2H-depletion through the growing season (Fig. 4). The *n*-C_{27}, *n*-C_{29}, and *n*-C_{31} alkanes in *C. argyi* have variations that are quite similar to those in *S. officinalis*. In contrast, the δ^2H values of *n*-alkanes in *E. esula* show a different pattern over the five sampling intervals, with more negative δ^2H values in the leaves collected in September. The surface peat deposits show a relatively narrow range in the δ^2H values of *n*-C_{27}, *n*-C_{29}, and *n*-C_{31} alkanes in different season (−206±7, −203±4 and −200±4, respectively; Fig. 4). These values are very similar to those in leaves collected in November.

4 Discussion

4.1 Turnover of leaf wax *n*-alkanes in the peat-forming species

Whether leaf wax *n*-alkane δ^2H values record environmental information for only a brief part of annual leaf growth or integrate information for the whole growing season remains an open question (e.g., Sachse et al., 2009, 2010; Kahmen et al., 2011; Tipple et al., 2013; Huang et al., 2018c). Some studies have proposed that leaf wax δ^2H values 'lock-in' environmental conditions only during

Table 2 The δ^2H values of peat source water (δ^2H_{sw}) and surface peat deposits *n*-alkanes (δ^2H_{27}, δ^2H_{29}, δ^2H_{31}) collected from the Dajiuhu peatland at May, July, September, and November 2014

	Source water			Surface peat deposit										
	δ^2H_{sw}/‰	$STD^{\#\#}_{\delta H_{sw}}$	$n^{\#\#\#}$	CPI	$STD^{\#\#}_{CPI}$	ACL	$STD^{\#\#}_{ACL}$	δ^2H_{27}/‰	$STD^{\#\#}_{\delta H_{27}}$	δ^2H_{29}/‰	$STD^{\#\#}_{\delta H_{29}}$	δ^2H_{31}/‰	$STD^{\#\#}_{\delta H_{31}}$	$n^{\#\#\#}$
May[#]	–29.4	9.5	15	6.1	0.8	29.9	0.9	–207	13.6	–204	8.9	–201	10.2	8
July	–43.7	9.6	26	5.8	1.0	29	1.0	–196	12.9	–199	13.9	–194	11.7	8
September	–72.4	5.1	26	5.3	0.9	29.2	0.8	–211	13.2	–208	9.1	–202	9.8	9
November	–72.7	3.7	26	5.2	1.0	29.3	1.0	–210	6.5	–200	16.7	–201	13.0	7

Notes: [#]: the δ^2H vaules of peat source water were not monitored in May 2014 and replaced the δ^2H values of surface peat deposits in May 2015 from Zhao et al. (2018); [##]: the standard deviation in different surface peat deposits; [###]: the number of water samples and surface peat deposits collected during each field trip.

the early stage of leaf growth (Sachse et al., 2010; Kahmen et al., 2011; Tipple et al., 2013). In contrast, Sachse et al. (2009) and Huang et al. (2018c) have argued that the δ^2H signal preserved in soils or sediments was an integrated value of the end of the growth period. Resolution of the seemingly contradictory interpretations may rest on knowing how fast the leaf wax regeneration rate is during leaf growth. Greenhouse experiments conducted by Gao et al. (2012a) have revealed that grass species probably have a relatively quicker regeneration rate of leaf waxes than tree species. One grass species (*Phleum pratense*) grown in the greenhouse exhibited a recycling time of two to four months for C_{27}-C_{31} *n*-alkyl lipids (Gao et al., 2012b). In contrast, the recycling time of long chain leaf wax in the tree species *Fraxinus americana* is lower by one to two orders of magnitude (Gao et al., 2012a). So the rapid lipid regeneration rates in grass species made it possible to disturb isotope assimilation over the whole growing season (Gao et al., 2014; Freimuth et al., 2017), while the isotope values of leaf wax in trees fluctuated in young leaves and were stable in mature leaves (Suh et al., 2018).

The seasonal variations of *n*-alkane concentration and compositions could provide evidence to answer whether or not the leaf wax δ^2H signal is 'locked-in' in a relatively short interval in the peat-forming species studied here. In this study, the total *n*-alkane concentration results suggest that the initial stage of leaf development is characterized by *de novo* synthesis (Huang et al., 2019). The decreasing trend of the total *n*-alkane concentration in the following months (until September) probably resulted from the dominance of removal of *n*-alkanes over deposition of new leaf waxes. At the growth end, both forb species (*S. officinalis* and *E. esula*) show an increase of the total *n*-alkane concentration, possibly resulting from the removal of chlorophyll and other leaf constituents during leaf senescence and thus the relative enrichment of *n*-alkanes in the bulk leaf material. Freimuth et al. (2017) coincidentally proved the point that the shift in plant metabolism and wax synthesis controlled the δ^2H variability in developing and mature leaves. This deduction is also supported by the ACL ratios. The near constant ACL values of the two forb species through the growth season suggest that removal does not affect the composition of long chain *n*-alkanes. The situation is more complex for the grass species (*C. argyi*), which shows a general decrease of the total *n*-alkane concentration and variable ACL values through the whole growing season.

We assume that the δ^2H compositions of surface peat water have similar seasonal patterns in different years, such as Zhao et al. (2018) 2015–2017 monitoring of surface peat water δ^2H ratios in Dajiuhu peatland. The peat water generally enriches in ^2H between May and July relative to September and November (Table 2). The trend of surface peat water δ^2H is consistent with the seasonal variations of δ^2H values of the long-chain *n*-alkanes. Such a close relation between leaf waxes and peat water δ^2H ratios may suggest that the regeneration of leaf waxes in peat-forming species is more rapid than indicated by previous studies (Huang et al., 2018a).

These results suggest that the initial stage of leaf flush is quite important for leaf wax synthesis in the herb species at the Dajiuhu peatland, which is consistent with previous studies (Sachse et al., 2010, 2015; Kahmen et al., 2011; Tipple et al., 2013). An important difference is that removal of *n*-alkanes may predominate over a longer interval than in the study of Sachse et al. (2015). Due to the seasonal variations of source water δ^2H ratios the renewed *n*-alkanes probably have different δ^2H compositions with the older ones. Hence, the composite δ^2H signals do not stay constant through the growing season. This interpretation is different from some of the previous studies on tree species (Kahmen et al., 2011; Tipple et al., 2013; Sachse et al., 2015), but it is consistent with the conclusions of Newberry et al. (2015). If we consider the continuous production of new leaf generations of barley studied by Sachse et al. (2010), an integration results from different generations will be recorded in the mature specimens of barley. Compared with trees, grasses can synthesize wax continuously through the growing season (Gulz and Muller, 1992; Gao et al., 2012a). Thus it is possible that grass and/or forb species integrate the environmental signals from quite long intervals into the leaf wax δ^2H ratios during their growth. However, this deduction requires results from more herb species and from wide climate conditions to validate.

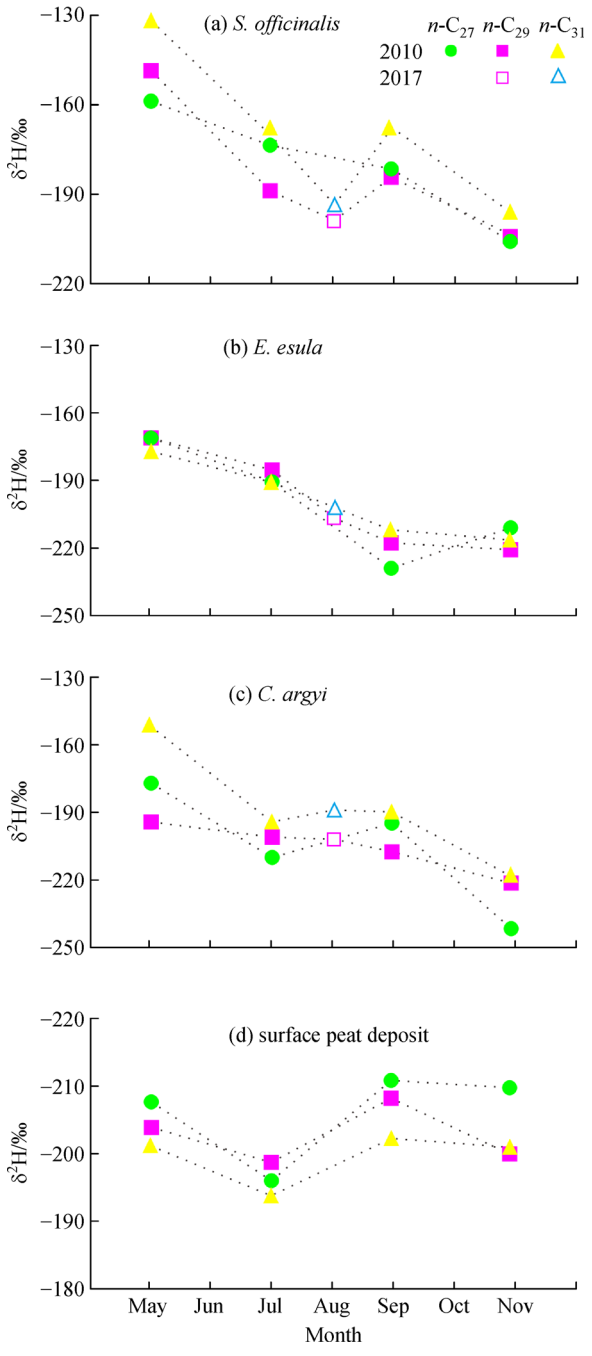

Fig. 4 Seasonal variations of δ^2H values of n-C_{27}, n-C_{29}, and n-C_{31} alkanes in the leaves of three plant species during 2010 and August 2017 (Huang et al., 2018a) and surface peat deposits during 2014.

We also need to consider the influence from the biosynthesis hydrogen isotope fractionation as documented by Newberry et al. (2015), which attributed the decreased trend of leaf wax δ^2H ratios in a growing season to the variation in biosynthetic fractionation. Different from the tree species studied by Newberry et al. (2015), the herb species investigated here only keep their belowground parts at the growing end. Thus the stored carbohydrates will have different influence on the leaf wax δ^2H ratios of the new-borne leaves between tree and herb species at the early stage of the growing season. In the Asian monsoon regions, the vapor source and the associated precipitation δ^2H ratios change seasonally (Johnson et al., 2004). The migration of vapor source probably exerts a more important effect on the leaf wax δ^2H ratios than the variation of biosynthesis fractionation (Huang et al., 2016, 2018a).

4.2 Association of environmental factors with *n*-alkane indexes

Previous studies have proposed that the ACL values have the potential to record climate changes (Schefuß et al., 2003; Bush and McInerney, 2013, 2015; Huang et al., 2016; Norström et al., 2017; Wang et al., 2018; Bai et al., 2019) and the succession of vegetation types (Liu et al., 2018). A persisting problem is to separate the relative importance of temperature from that of relative humidity on the ACL values (Bai et al., 2019). In this study, because our data are limited to four sampling intervals in one year, it is difficult to evaluate the relative importance of temperature relative to precipitation in affecting the *n*-alkane compositions of these plants in this setting. In addition, possible turnover of leaf waxes might complicate the relation between *n*-alkane ratios and climatic parameters. However, it is clear that the ACL values of two dicotyledons (*S. officinalis* and *E. esula*) and monocotyledons (C. *argyi*) are significantly different in all sampling intervals (Fig. 3). An extensive investigation of terrestrial higher plant leaf waxes in the central Chinese Loess Plateau showed that the ACL value were a good indicator for distinguishing dicotyledons and monocotyledons (Liu et al., 2018). But combined with the results of our study and Zhao et al. (2018) in the Dajiuhu peatland, the average ACL value of dicotyledonous leaves is smaller than that of monocotyledonous leaves. The different ACL values of dicotyledonous and monocotyledonous in the Dajiuhu peatland and Chinese Loess Plateau may be caused by different limiting factors or different response strategies to water use of plant growth between humid area and arid area (Huang et al., 2018a; Liu et al., 2018).

Besides ACL index, the δ^2H_{alk} and the $\varepsilon_{alk/sw}$ values are also good indicators to distinguish environmental factors and vegetation communities (Sachse et al., 2012; Liu et al., 2016, 2021a, 2021b; Session et al., 2016; Huang et al., 2018a). Liu et al. (2016) reported that the δ^2H_{alk} of the monocotyledonous was more ^{2}H-depleted than the δ^2H_{alk} of the dicotyledonous. The main reason was that the leaves of these two types of plants had different venation distribution which controls the hydrogen isotopes fractionation process of water in leaves (Helliker et al., 2000; Liu et al., 2021b). But the average δ^2H_{alk} of two dicotyledons (*S. officinalis* and *E. esula*) and monocotyledons (C. *argyi*) in our study showed no significant

Table 3 The correlation efficiency between the δ^2H_{sw}, δ^2H_{alk}, $\varepsilon_{alk/sw}$, and environmental factors (MAT and MMP)

		Sanguisorba officinalis			*Euphorbia esula*			*Carex argyi*			Surface peat deposit			Source water
		δ^2H_{27}	δ^2H_{29}	δ^2H_{31}	δ^2H_{27}	δ^2H_{29}	δ^2H_{31}	δ^2H_{27}	δ^2H_{29}	δ^2H_{31}	δ^2H_{27}	δ^2H_{29}	δ^2H_{31}	δ^2H_{sw}
MAT	*r*	0.69	0.33	0.50	0.14	0.47	0.46	0.62	0.71	0.42	0.61	-0.22	0.55	0.42
	p	0.31	0.69	0.50	0.86	0.53	0.54	0.38	0.29	0.52	0.34	0.78	0.45	0.58
MMP	*r*	**0.96**	0.73	0.85	0.56	0.81	0.82	0.85	**0.97**	0.78	0.55	-0.21	0.41	0.78
	p	**0.04**	0.27	0.15	0.44	0.19	0.18	0.15	**0.03**	0.21	0.45	0.79	0.59	0.22
		Sanguisorba officinalis			*Euphorbia esula*			*Carex argyi*			Surface peat deposit			
		$\varepsilon_{27/sw}$	$\varepsilon_{29/sw}$	$\varepsilon_{31/sw}$	$\varepsilon_{27/sw}$	$\varepsilon_{29/sw}$	$\varepsilon_{31/sw}$	$\varepsilon_{27/sw}$	$\varepsilon_{29/sw}$	$\varepsilon_{31/sw}$	$\varepsilon_{27/sw}$	$\varepsilon_{29/sw}$	$\varepsilon_{31/sw}$	
MAT	*r*	0.59	0.01	0.46	–0.45	0.59	0.48	0.46	0.08	0.24	–0.15	–0.22	–0.13	
	p	0.41	0.99	0.54	–0.56	0.41	0.52	0.54	0.92	0.77	0.42	0.22	0.48	
MMP	*r*	0.41	0.18	0.69	0.06	0.89	0.46	0.44	–0.31	0.43	**–0.52**	**–0.59**	**–0.52**	
	p	0.59	0.82	0.31	0.94	0.11	0.55	0.56	0.69	0.57	**0.00**	**0.00**	**0.00**	

difference with one-way ANOVA tests (p = 0.33). This consistency shows that the fluctuations of the δ^2H_{alk} values in these plants are affected by some common environmental factors rather than by those that are species-dependent (Balascio et al., 2018; Huang et al., 2018a). Although our data for each plant are relatively limited, we can still explore the relationship between δ^2H_{alk} and climatic parameters using the monthly mean values for air temperature (MAT) and precipitation (MMP). The δ^2H_{alk} values show a weak correlation with both MAT and MMP (Table 3). In some cases, the p values are lower than 0.05.

In this study, the three plant species show quite similar trends of the $\varepsilon_{alk/sw}$ values compared with their δ^2H values of *n*-C_{27}, *n*-C_{29}, and *n*-C_{31} alkanes along with the growing season (Fig. 5). The δ^2H values had higher correlation efficiency with environmental factors (MAT and MMP) than the $\varepsilon_{alk/sw}$ values in three plants (Table 3). So the different biosynthetic fractionation factors may be mostly derived from different hydrogen sources during lipid synthesis and environmental factors (Liu et al., 2016). The hydrogen isotope fractionation between source water and lipids may result from evaporation of the peat water (Huang et al., 2018a). As noted by Duan et al. (2013), the δ^2H_{alk} values of a variety of different plants are related to the isotopic composition of their environmental water. Alternatively, the observed patterns of $\varepsilon_{alk/sw}$ through the growing course (Fig. 5) are possibly a biosynthetic response of peat-forming plants (Sachse et al., 2015).

4.3 Implications of paleohydrological applications

In peatlands, *in situ* vegetation contributes most of the organic matter (Farrimond and Flanagan, 1996). If the turnover rate of long chain *n*-alkanes in the Dajiuhu peatland is as fast as *P. pratense* growing in the greenhouse as found by Gao et al. (2012b) or is on the order of weeks as reported by Sachse et al. (2009), variations in the environmental conditions along with the plant growth will be integrated into the δ^2H signals of plant litter and finally preserved in peat deposits. Nonetheless, we must also consider the possible contribution of lipids from plant roots, which can be an important source of organic matter in some peat-forming conditions (Rydin and Jeglum, 2006). One of our earlier studies investigated the wax lipids in the roots collected from the Dajiuhu peatland in June 2009 (Huang et al., 2011). That work revealed that in most plant samples, the concentration of major lipid groups (i.e., long chain *n*-alkanes, *n*-fatty alcohols) was at least one order of magnitude lower in roots than in their above-ground leafy counterparts (Liu et al., 2019; He et al., 2020). Thus in the Dajiuhu peatland, leaves probably make a more important contribution than roots to the long chain *n*-alkanes preserved in peat horizons. Taking into consideration the seasonal variations of the δ^2H_{alk} of three peat-forming plants and comparing with the δ^2H_{alk} values of the peat deposits, it is likely that that leaf wax δ^2H_{alk} values in peat deposits record environmental information from the end of the annual growth period rather than an average of the whole growth season.

If the above deduction is proven to be valid in herb-dominated peatlands like Dajiuhu (Zhao et al., 2018; Huang et al., 2018a) and also the Zoigê peatland that was studied by Seki et al. (2011), it would be interesting to investigate leaf wax δ^2H_{alk} values in peatlands like Hani that was studied by Seki et al. (2009) where some tree species contribute to the peat accumulations (Bu et al., 2011). In the latter case, study of leaf wax δ^2H_{alk} values from different kinds of plants (e.g., herbs, trees, mosses) may reveal novel environmental information from the different parts of the growing season that is recorded by the different plant types (Huang et al., 2018a; Xia et al., 2020) or the habitat of these plants (Bai et a., 2015; Yan et al., 2020; Yang and Huang, 2020). In conclusion, in wetland environments, plant types are mainly controlled by inter-annual water regime variation (Shen et al., 2020), the hydrogen isotope signals of leaf *n*-alkane in plants, and sediment record secondary hydrogen isotope of variation in seasonal water conditions.

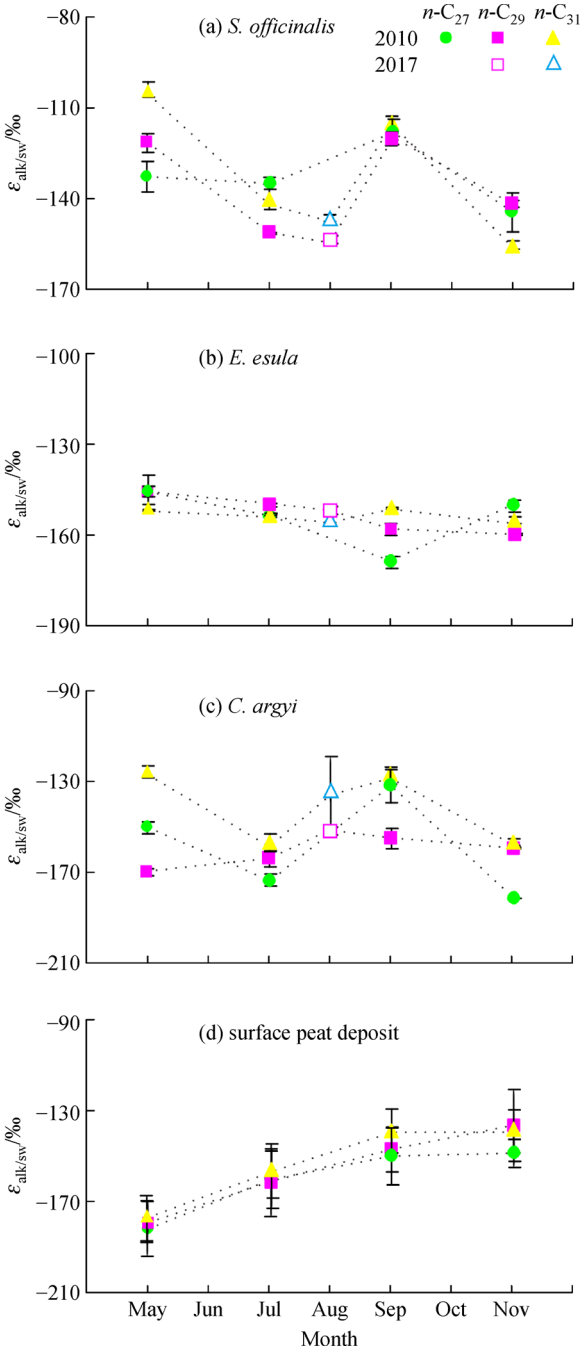

Fig. 5 Seasonal variations of $\varepsilon_{alk/sw}$ in the leaves of three plant species during 2010 and August 2017 (Huang et al., 2018a) and surface peat deposits during 2014.

5 Conclusions

We investigated the molecular distributions and hydrogen isotopic compositions of long chain *n*-alkanes in three dominant peat-forming vascular plant species collected over the growing season in the Dajiuhu peatland. Both total alkane concentrations and molecular ratios (CPI and ACL) show obvious variations during plant growth. Young leaves have CPI values that can reach as high as 50 in May. The leaf CPI values decrease during the summer and finally show a moderate increase from September to the senescent and withered leaf stage in November. The ACL values of the three species display a moderate increase from the young leaves in May to the mature leaves in July. Like the CPI values, the ACL values increase from September to November.

The δ^2H values of long chain *n*-alkanes show a general decreasing trend through the whole growth season, with the values in the withered leaves quite similar to those in the surface peats collected at the same site in the Dajiuhu peatland. Combining the results of our measurements of alkane concentration and δ^2H values, it is likely that *de novo* synthesis of leaf wax *n*-alkanes in the peat-forming plant species is mainly during the early stage of leaf development, and the renewal of *n*-alkanes in the following months modifies their initial hydrogen isotope compositions during the growing season. Consequently, the leaf wax δ^2H ratios integrate the environmental variations at the end of plant growth period (usually in the autumn) rather than the whole period or the earth growth period for these peat-forming vascular plant species.

Acknowledgements This work was supported by the National Natural Foundation of China (Grant No. 41903066) and the scientific research funds for universities (No. X19G028). Xianyu Huang, Philip A. Meyers and Haoxin Fan are thanked for their useful comments and English modification that improved the early version of the manuscript. Jinxiang Zhang and Weichao Wu are thanked for helping in the sample collection and lipid treatments. Dr. Yangmin Qin, Xinxin Wang and Prof. Hongmei Wang are acknowledged for their help during the field trips.

References

Andersson R A, Meyers P A, Hornibrook E, Kuhry P, Mörth C M (2012). Elemental and isotopic carbon and nitrogen records of organic matter accumulation in a Holocene permafrost peat sequence in the East European Russian Arctic. J Quat Sci, 27(6): 545–552

Baas M, Pancost R, van Geel B, Sinninghe Damsté J S (2000). A comparative study of lipids in *Sphagnum* species. Org Geochem, 31(6): 535–541

Bai Y, Fang X, Jia G, Sun J, Wen R, Ye Y (2015). Different altitude effect of leaf wax *n*-alkane δD in surface soils along two vapor transport pathways, southeastern Tibetan Plateau. Geochim Cosmochim Acta, 170: 94–107

Bai Y, Azamdzhon M, Wang S, Fang X, Guo H, Zhou P, Chen C, Liu X, Jia S, Wang Q (2019). An evaluation of biological and climatic effects on plant *n*-alkane distributions and δ^2H_{alk} in a field experiment conducted in central Tibet. Org Geochem, 135: 53–63

Balascio N L, D'Andrea W J, Anderson R S, Wickler S (2018). Influence of vegetation type on *n*-alkane composition and hydrogen isotope values from a high latitude ombrotrophic bog. Org Geochem, 121: 48–57

Bingham E M, McClymont E L, Väliranta M, Mauquoy D, Roberts Z, Chambers F M, Pancost R D, Evershed R P (2010). Conservative

composition of *n*-alkane biomarkers in *Sphagnum* species: implications for palaeoclimate reconstruction in ombrotrophic peat bogs. Org Geochem, 41(2): 214–220

Blackford J (2000). Palaeoclimatic records from peat bogs. Trends Ecol Evol, 15(5): 193–198

Bu Z J, Rydin H, Chen X (2011). Direct and interaction-mediated effects of environmental changes on peatland bryophytes. Oecologia, 166 (2): 555–563

Bush R T, McInerney F A (2013). Leaf wax *n*-alkane distributions in and across modern plants: implications for paleoecology and chemotaxonomy. Geochim Cosmochim Acta, 117: 161–179

Bush R T, McInerney F A (2015). Influence of temperature and C_4 abundance on *n*-alkane chain length distributions across the central USA. Org Geochem, 79: 65–73

Chambers F M, Booth R K, De Vleeschouwer F, Lamentowicz M, Le RouxG, Mauquoy D, Nichols J E, van Geel B (2012). Development and refinement of proxy-climate indicators from peats. Quat Int, 268: 21–33

Chikaraishi Y, Naraoka H (2006). Carbon and hydrogen isotope variation of plant biomarkers in a plant-soil system. Chem Geol, 231(3): 190–202

Cisneros-Dozal L M, Heikoop J M, Fessenden J, Anderson R S, Meyers P A, Allen C D, Hess M, Larson T, Perkins G, Rearick M (2010). A 15000-year record of climate change in northern New Mexico, USA, inferred from isotopic and elemental contents in bog sediments. J Quat Sci, 25(6): 1001–1007

Duan Y, Wu Y, Cao X, Yang Z, Ma L (2014). Hydrogen isotope ratios of individual *n*-alkanes in plants from Gannan Gahai Lake (China) and surrounding area. Org Geochem, 77: 96–105

Farrimond P, Flanagan R L (1996). Lipid stratigraphy of a Flandrian peat bed (Northumberland, UK): comparison with the pollen record. Holocene, 6(1): 69–74

Freimuth E, Diefendorf A, Lowell T V (2017). Hydrogen isotopes of *n*-alkanes and *n*-alkanoic acids as tracers of precipitation in a temperate forest and implications for paleorecords. Geochim Cosmochim Acta, 206: 166–183

Freimuth E, Diefendorf A, Lowell T V, Wiles G C (2019). Sedimentary *n*-alkanes and *n*-alkanoic acids in a temperate bog are biased toward woody plants. Org Geochem, 128: 94–107

Gao L, Burnier A, Huang Y (2012a). Quantifying instantaneous regeneration rates of plant leaf waxes using stable hydrogen isotope labeling. Rapid Commun Mass Sp, 26(2): 115–122

Gao L, Tsai Y J, Huang Y (2012b). Assessing the rate and timing of leaf wax regeneration in *Fraxinus americana* using stable hydrogen isotope labeling. Rapid Commun Mass Sp, 26(19): 2241–2250

Gao L, Edwards E J, Zeng Y, Huang Y (2014). Major evolutionary trends in hydrogen isotope fractionation of vascular plant leaf waxes. PLoS One, 9(11): e112610

Gogo S, Laggoun-Défarge F, Merzouki F, Mounier S, Guirimand-Dufour A, Jozja N, Huguet A, Delarue F, Défarge C (2016). In situ and laboratory non-additive litter mixture effect on C dynamics of *sphagnum rubellum* and *molinia caerulea* litters. J Soils Sediments, 16(1): 13–27

Gülz P G, Muller E (1992). Seasonal variation in the composition of epicuticular waxes of *Quercus robur* leaves. Z Naturforsch C, 47(11–12): 800–806

He D, Nemiah Ladd S, Saunders C J, Mead R N, Jaffé R (2020). Distribution of *n*-alkanes and their δ^2H and δ^{13}C values in typical plants along a terrestrial-coastal-oceanic gradient. Geochim Cosmochim Acta, 281: 31–52

Helliker B R, Ehleringer J R (2000). Establishing a grassland signature in veins: ^{18}O in the leaf water of C_3 and C_4 grasses. Proc Natl Acad Sci USA, 97(14): 7894–7898

Herrera-Herrera A V, Leierer L, Jambrina-Enríquez M, Connolly R, Mallol C (2020). Evaluating different methods for calculating the carbon preference index (CPI): implications for palaeoecological and archaeological research. Org Geochem, 146: 104056

Hong Y, Wang Z, Jiang H, Lin Q, Hong B, Zhu Y, Wang Y, Xu L, Leng X, Li H (2001). A 6000-year record of changes in drought and precipitation in northeastern China based on a δ^{13}C time series from peat cellulose. Earth Planet Sci Lett, 185(1–2): 111–119

Huang X, Wang C, Zhang J, Wiesenberg G L B, Zhang Z, Xie S (2011). Comparison of free lipid compositions between roots and leaves of plants in the Dajiuhu Peatland, Central China. Geochem J, 45(5): 365–373

Huang X, Xue J, Meyers P A, Gong L, Wang X, Liu Q, Qin Y, Wang H (2014). Hydrologic influence on the δ^{13}C variation in long chain *n*-alkanes in the Dajiuhu peatland, central China. Org Geochem, 69: 114–119

Huang X, Meyers P A, Xue J, Zhang Y, Wang X (2016). Paleoclimate significance of *n*-alkane molecular distributions and δ^2H values in surface peats across the monsoon region of China. Palaeogeogr Palaeoclimatol Palaeoecol, 461: 77–86

Huang X, Meyers P A (2018a). Assessing paleohydrologic controls on the hydrogen isotope compositions of leaf wax *n*-alkanes in chinese peat deposits. Palaeogeogr Palaeoclimatol Palaeoecol, 516: 354–363

Huang X, Pancost R D, Xue J, Gu Y, Evershed R P, Xie S (2018b). Response of carbon cycle to drier conditions in the mid-Holocene in central China. Nat Commun, 9(1): 1369

Huang X, Zhao B, Wang K, Hu Y, Meyers P A (2018c). Seasonal variations of leaf wax *n*-alkane molecular composition and δD values in two subtropical deciduous tree species: results from a three-year monitoring program in central China. Org Geochem, 118: 15–26

Johnson K R, Ingram B L (2004). Spatial and temporal variability in the stable isotope systematics of modern precipitation in China: implications for paleoclimate reconstructions. Earth Planet Sci Lett, 220(3–4): 365–377

Kahmen A, Dawson T E, Vieth A, Sachse D (2011). Leaf wax *n*-alkane δD values are determined early in the ontogeny of *Populus trichocarpa* leaves when grown under controlled environmental conditions. Plant Cell Environ, 34(10): 1639–1651

Kahmen A, Schefuß E, Sachse D (2013a). Leaf water deuterium enrichment shapes leaf wax *n*-alkane δD values of angiosperm plants I: experimental evidence and mechanistic insights. Geochim Cosmochim Acta, 111: 39–49

Kahmen A, Hoffmann B, Schefuß E, Arndt S K, Cernusak L A, West J B, Sachse D (2013b). Leaf water deuterium enrichment shapes leaf wax *n*-alkane δD values of angiosperm plants II: observational evidence and global implications. Geochim Cosmochim Acta, 111: 50–63

Liu H, Gu Y, Yu Z, Huang C, Ge J, Huang X, Xie S, Zheng M, Zhang Z, Cheng S (2020). Holocence peatland water regulation response to

1000-year solar cycle indicated by phytoliths in central China. J Hydrol (Amst), 589: 125169

Liu J, Liu W, An Z, Yang H (2016). Different hydrogen isotope fractionations during lipid formation in higher plants: implications for paleohydrology reconstruction at a global scale. Sci Rep, 6(1): 19711

Liu J, An Z, Wang Z, Wu H (2017). Using $\delta D_{n\text{-alkane}}$ as a proxy for paleo-environmental reconstruction: a good choice to sample at the site dominated by woods. Sci Total Environ, 599-600: 554–559

Liu J, An Z, Liu H (2018). Leaf wax *n*-alkane distributions across plant types in the central Chinese Loess Plateau. Org Geochem, 125: 260–269

Liu J, An Z, Wu H, Yu Y (2019). Comparison of *n*-alkane concentrations and δD values between leaves and roots in modern plants on the Chinese Loess Plateau. Org Geochem, 138: 103913

Liu J (2021a). Seasonality of the altitude effect on leaf wax *n*-alkane distributions, hydrogen and carbon isotopes along an arid transect in the Qinling Mountains. Sci Total Environ, 778: 146272

Liu J, An Z, Lin G (2021b). Intra-leaf heterogeneities of hydrogen isotope compositions in leaf water and leaf wax of monocots and dicots. Sci Total Environ, 770: 145258

Luo P, Peng P, Lü H, Zheng Z, Wang X (2012). Latitudinal variations of CPI values of long-chain *n*-alkanes in surface soils: evidence for CPI as a proxy of aridity. Sci China Earth Sci, 55(7): 1134–1146

Luo T, Lun Z, Gu Y, Qin Y, Zhang Z, Zhang B (2015). Plant community survey and ecological of Dajiuhu Wetland in Shennongjia Area. Wetland Sci, 13: 153–160 (in Chinese)

Marzi R, Torkelson B E, Olson R K (1993). A revised carbon preference index. Org Geochem, 20(8): 1303–1306

Newberry S L, Kahmen A, Dennis P, Grant A (2015). *n*-Alkane biosynthetic hydrogen isotope fractionation is not constant throughout the growing season in the riparian tree *Salix viminalis.* Geochim Cosmochim Acta, 165: 75–85

Nichols J, Booth R K, Jackson S T, Pendall E G, Huang Y (2010). Differential hydrogen isotopic ratios of *Sphagnum* and vascular plant biomarkers in ombrotrophic peatlands as a quantitative proxy for precipitation-evaporation balance. Geochim Cosmochim Acta, 74(4): 1407–1416

Nichols J E, Booth R K, Jackson S T, Pendall E G, Huang Y (2006). Paleohydrologic reconstruction based on *n*-alkane distributions in ombrotrophic peat. Org Geochem, 37(11): 1505–1513

Nichols J E, Huang Y (2012). Hydroclimate of the northeastern United States is highly sensitive to solar forcing. Geophys Res Lett, 39(4): L04707

Nichols J E, Peteet D M, Moy C M, Castanêda I S, McGeachy A, Perez M (2014). Impacts of climate and vegetation change on carbon accumulation in a south-central Alaskan peatland assessed with novel organic chemical techniques. Holocene, 24(9): 1146–1155

Norström E, Katrantsiotis C, Smittenberg R H, Kouli K (2017). Chemotaxonomy in some Mediterranean plants and implications for fossil biomarker records. Geochim Cosmochim Acta, 219: 96–110

Nott C J, Xie S, Avsejs L A, Maddy D, Chambers F M, Evershed R P (2000). n-Alkane distributions in ombrotrophic mires as indicators of vegetation change related to climatic variation. Org Geochem, 31(2-3): 231–235

Ortiz J E, Gallego J L R, Torres T, Díaz-Bautista A, Sierra C (2010). Palaeoenvironmental reconstruction of Northern Spain during the last 8000 calyr BP based on the biomarker content of the Roñanzas peat bog (Asturias). Org Geochem, 41(5): 454–466

Pancost R D, Baas M, van Geel B, Sinninghe Damsté J S (2002). Biomarkers as proxies for plant inputs to peats: an example from a sub-boreal ombrotrophic bog. Org Geochem, 33(7): 675–690

Pedentchouk N, Sumner W, Tipple B, Pagani M (2008). δ^{13}C and δD compositions of *n*-alkanes from modern angiosperms and conifers: an experimental set up in central Washington State, USA. Org Geochem, 39(8): 1066–1071

Poynter J G, Farnimond P, Robinson N, Eglinton G (1989). Aeolian-derived higher plant lipids in the marine sedimentary record: links with palaeoclimate. Paleoclimatology and Paleometeorology. In: Leinen M, Sarnthein M, eds. Paleoclimatology and Paleometeorology: Modern and Past Patterns of Global Atmospheric Transport: 435–462

Qin Y, Payne R J, Gu Y, Huang X, Wang H (2012). Ecology of testate amoebae in Dajiuhu peatland of Shennongjia Mountains, China, in relation to hydrology. Front Earth Sci, 6(1): 57–65

Rao Z, Wu Y, Zhu Z, Jia G, Henderson A (2011). Is the maximum carbon number of long-chain *n*-alkanes an indicator of grassland or forest? Evidence from surface soils and modern plants. Chin Sci Bull, 56(16): 1714–1720

Rao Z, Zhu Z, Wang S, Jia G, Qiang M, Wu Y (2009). CPI values of terrestrial higher plant-derived long-chain *n*-alkanes: a potential paleoclimatic proxy. Front Earth Sci, 3(3): 266–272

Rydin H, Jeglum J K (2006). The Biology of Peatlands. New York: Oxford University Press

Sachse D, Billault I, Bowen G J, Chikaraishi Y, Dawson T, Feakins S J, Freeman K H, Magill C R, McInerney F A, van der Meer M T J, Polissar P, Robins R, Sachs J P, Schmidt H L, Sessions A L, White J W C, West J B, Kahmen A (2012). Molecular paleohydrology: interpreting the hydrogen-isotopic composition of lipid biomarkers from photosynthesizing organisms. Annu Rev Earth Planet Sci, 40 (1): 221–249

Sachse D, Gleixner G, Wilkes H, Kahmen A (2010). Leaf wax *n*-alkane δD values of field-grown barley reflect leaf water δD values at the time of leaf formation. Geochim Cosmochim Acta, 74(23): 6741–6750

Sachse D, Kahmen A, Gleixner G (2009). Significant seasonal variation in the hydrogen isotopic composition of leaf-wax lipids for two deciduous tree ecosystems (*Fagus sylvativa* and *Acer pseudoplatanus*). Org Geochem, 40(6): 732–742

Sachse D, Dawson T E, Kahmen A (2015). Seasonal variation of leaf wax *n*-alkane production and δ^2H values from the evergreen oak tree, *Quercus agrifolia.* Isotopes Environ Health Stud, 51(1): 124–142

Schefuß E, Ratmeyer V, Stuut J B W, Jansen J H, Sinninghe Damsté J S (2003). Carbon isotope analyses of *n*-alkanes in dust from the lower atmosphere over the Central Eastern Atlantic. Geochim Cosmochim Acta, 67(10): 1757–1767

Seki O, Meyers P A, Kawamura K, Zhou W, Zheng Y (2009). Hydrogen isotopic ratios of plant-wax *n*-alkanes in a peat bog deposited in northeastern China during the last 16 kyr. Org Geochem, 40(6): 671–677

Seki O, Meyers P A, Yamamoto S, Kawamura K, Nakatsuka T, Zhou W, Zheng Y (2011). Plant-wax hydrogen isotopic evidence for

postglacial variations in delivery of precipitation in the monsoon domain of China. Geology, 39(9): 875–878

Sessions A L (2006). Seasonal changes in D/H fractionation accompanying lipid biosynthesis in *Spartina alterniflora.* Geochim Cosmochim Acta, 70(9): 2153–2162

Sessions A L (2016). Factors controlling the deuterium contents of sedimentary hydrocarbons. Org Geochem, 96: 43–64

Shen R, Lan Z, Huang X, Chen Y, Hu Q, Fang C, Jin B, Chen J (2020). Soil and plant characteristics during two hydrologically contrasting years at the lakeshore wetland of Poyang Lake, China. J Soils Sediments, 20(9): 3368–3379

Song L, Li H, Wang K, Wu D, Wu H (2014). Ecology of testate amoebae and their potential use as palaeohydrologic indicators from peatland in Sanjiang Plain, northeast China. Front Earth Sci, 8(4): 564–572

Suh Y J, Diefendorf A F (2018). Seasonal and canopy height variation in *n*-alkanes and their carbon isotopes in a temperate forest. Org Geochem, 116: 23–34

Tipple B J, Berke M A, Doman C E, Khachaturyan S, Ehleringer J R (2013). Leaf-wax *n*-alkanes record the plant-water environment at leaf flush. Proc Natl Acad Sci USA, 110(7): 2659–2664

Wang J, Xu Y, Zhou L, Shi M, Axia E, Jia Y, Chen Z, Li J, Wang G (2018). Disentangling temperature effects on leaf wax *n*-alkane traits and carbon isotopic composition from phylogeny and precipitation. Org Geochem, 126: 13–22

Xia Z, Zheng Y, Stelling J M, Loisel J, Huang Y, Yu Z (2020). Environmental controls on the carbon and water (H and O) isotopes in peatland *Sphagnum* mosses. Geochim Cosmochim Acta, 277: 265–284

Xie S, Nott C J, Avsejs L A, Volders F, Maddy D, Chambers F M, Gledhill A, Carter J F, Evershed R P (2000). Palaeoclimate records in compound-specific δD values of a lipid biomarker in ombrotrophic peat. Org Geochem, 31(10): 1053–1057

Yan C, Zhang Y, Zhang Y, Zhang Z, Huang X (2020). Habitat influence on the molecular, carbon and hydrogen isotope compositions of leaf wax *n*-Alkanes in a subalpine basin, central China. J Earth Sci, 31(4): 845–852

Yang X, Huang X (2020). Different patterns of molecular, carbon and hydrogen isotope compositions of *n*-alkanes between heterotrophic plant and its hosts. Front Earth Sci, 14(4): 783–788

Yu S, Kang Z, Zhou W (2012). Quantitative palaeoclimate reconstruction as an inverse problem: a bayesian inference of Late-Holocene climate on the Eastern Tibetan Plateau from a peat cellulose δ^{18}O record. Holocene, 22(4): 405–412

Zhao B, Zhang Y, Huang X, Qiu R, Zhang Z, Meyers P A (2018). Comparison of *n*-alkane molecular, carbon and hydrogen isotope compositions of different types of plants in the Dajiuhu peatland, central China. Org Geochem, 124: 1–11

Zheng Y, Singarayer J S, Cheng P, Yu X, Liu Z, Valdes P J, Pancost R D (2014). Holocene variations in peatland methane cycling associated with the Asian summer monsoon system. Nat Commun, 5(1): 4631

Zhou W, Xie S, Meyers P A, Zheng Y (2005). Reconstruction of late glacial and Holocene climate evolution in southern China from geolipids and pollen in the Dingnan peat sequence. Org Geochem, 36 (9): 1272–1284